




## Article

# Indoor Air Quality in Cob Buildings: In Situ Studies and Artificial Neural Network Modeling

Karim Touati <sup>1,2,\*</sup> , Mohammed-Hichem Benzaama <sup>2,3</sup>, Yassine El Mendili <sup>2,3</sup> , Malo Le Guern <sup>2</sup> , François Streiff <sup>4</sup> and Steve Goodhew <sup>5</sup>

<sup>1</sup> EPF Ecole d'Ingénieurs, 21 Boulevard Berthelot, 34000 Montpellier, France

<sup>2</sup> Builders Ecole d'Ingénieurs, ComUE Normandie Université, 1 Rue Pierre et Marie Curie, 14610 Epron, France; hbenzaama@estp-paris.eu (M.-H.B.); yelmendili@estp-paris.eu (Y.E.M.); malo.leguern@builders-ingenieurs.fr (M.L.G.)

<sup>3</sup> Institut de Recherche de l'ESTP, Ecole Spéciale des Travaux Publics, 28 Avenue du Président Wilson, 94234 Cachan, France

<sup>4</sup> Parc Naturel Régional des Marais du Cotentin et du Bessin, 50500 Carentan-les-Marais, France; fstreiff@parc-cotentin-bessin.fr

<sup>5</sup> School of Art, Design and Architecture, University of Plymouth, Plymouth PL4 8AA, UK; s.goodhew@plymouth.ac.uk

\* Correspondence: karim.touati@epf.fr; Tel.: +33-4-99-65-99-55

**Abstract:** Knowledge of indoor air quality (IAQ) in cob buildings during the first few months following their delivery is of vital importance in preventing occupants' health problems. The present research focuses on evaluating IAQ in cob buildings through a prototype built in Normandy, France. To achieve this, the prototype was equipped with a set of sensors to monitor various parameters that determine indoor and outdoor air quality. These parameters include relative humidity (RH), carbon dioxide (CO<sub>2</sub>), nitrogen dioxide (NO<sub>2</sub>), ozone (O<sub>3</sub>), particulate matter (PM1 and PM10), and volatile organic compounds (VOCs). The obtained experimental results indicate that, overall, there is good indoor air quality in the prototype building. However, there are some noteworthy findings, including high indoor RH and occasional spikes in CO<sub>2</sub>, PM1, PM10, and VOCs concentrations. The high RH is believed to be a result of the ongoing drying process of the cob walls, while the peaks in pollutants are likely to be attributed to human presence and the earthen floor deterioration. To ensure consistent good air quality, this study recommends the use of a properly sized Controlled Mechanical Ventilation system. Additionally, this study explored IAQ in the cob building from a numerical perspective. A Long Short-Term Memory (LSTM) model was developed and trained to predict pollutant concentrations inside the building. A validation test was conducted on the CO<sub>2</sub> concentration data collected on-site, and the results indicated that the LSTM model has accurately predicted the evolution of CO<sub>2</sub> concentration within the prototype building over an extended period.

**Keywords:** indoor air quality; cob; light earth; carbon dioxide; artificial neural network



**Citation:** Touati, K.; Benzaama, M.-H.; El Mendili, Y.; Le Guern, M.; Streiff, F.; Goodhew, S. Indoor Air Quality in Cob Buildings: In Situ Studies and Artificial Neural Network Modeling. *Buildings* **2023**, *13*, 2892. <https://doi.org/10.3390/buildings13112892>

Academic Editor: Wei Liu

Received: 13 October 2023

Revised: 6 November 2023

Accepted: 16 November 2023

Published: 19 November 2023



**Copyright:** © 2023 by the authors. Licensee MDPI, Basel, Switzerland. This article is an open access article distributed under the terms and conditions of the Creative Commons Attribution (CC BY) license (<https://creativecommons.org/licenses/by/4.0/>).

## 1. Introduction

Indoor air quality (IAQ) is a critical concern for public health, especially in urban areas where people spend the majority of their time indoors [1,2]. Exposure to indoor air pollution can present significant health and productivity impacts. Several factors can influence IAQ within buildings, including outdoor pollution, ventilation systems, furniture, and human activities. To address this issue, effective methods and tools are needed to evaluate IAQ and ensure the well-being of building occupants [3,4]. Research has highlighted the importance of IAQ standards and certifications. Studies have compared IAQ requirements set by various building standards and found that pollutants such as formaldehyde, benzene, carbon dioxide, particulate matter, and radon are commonly considered in IAQ standards [5]. The need for health-level standards to address epidemic prevention has also been emphasized.

The effectiveness of green buildings in improving IAQ and reducing energy consumption has been studied. Green office buildings with one-to-three-star ratings were found to have superior IAQ compared to ordinary buildings, with lower concentrations of carbon dioxide and particulate matter [6]. However, the concentration of total Volatile Organic Compounds (VOCs) was higher in green buildings. These findings underscore the importance of assessing IAQ in green buildings to evaluate their impact on indoor air quality and energy consumption. IAQ requirements have been reviewed in various green building certifications worldwide, with VOCs, formaldehyde, and carbon dioxide being the most frequently considered indoor air pollutants [7]. Emission source control, ventilation, and indoor air measurement are the primary pathways used in green building schemes for IAQ management.

In the United States, IAQ, in a Leadership in Energy & Environmental Design (LEED)-certified green building, is regularly evaluated on an annual basis to ensure that indoor air pollutants remain within safe limits [8]. The assessment of such buildings has revealed several advantages in terms of air quality compared to conventional buildings. While the green building concept incorporates measures such as increased fresh air supply and the use of safe materials to address IAQ during the design phase, there is a scarcity of experimental data confirming IAQ improvements during the operational phase.

Regarding earthen architecture, it is important to note that there is a paucity of studies dealing with the effect of such vernacular techniques on a building's IAQ under living conditions. One of the noteworthy features of such buildings is their non-containment of Volatile Organic Compounds (VOCs), in stark contrast to many other construction materials like paint, adhesives, and sealants. These VOCs can significantly impact health and pose risks to building occupants throughout their lifetime [9]. Also, indoor air quality is directly linked to indoor relative humidity levels [10] and, therefore, earth's ability to passively regulate moisture levels could be beneficial for the occupants' health. Moreover, clay particles present in these materials can help remove pollutants due to their passive removal properties [11].

Despite the many advantages of cob construction, including hygrothermal comfort and low environmental impact, indoor air quality in this type of building has not been sufficiently studied, especially during the first few months following building delivery. Many studies have focused on other building types, such as concrete or timber structures, leaving the potential benefits or risks of cob construction relatively unknown. The present work attempts to fill this gap by collecting indoor air pollutants concentrations and investigating the IAQ of a cob building during the first few months following its delivery.

Elsewhere, advancements in digital technologies have led to the development of computational methods and tools for assessing IAQ. Computational Fluid Dynamics (CFD) simulations can provide insights into airflow patterns and pollutant dispersion within buildings. Machine learning and deep learning models can predict IAQ parameters and optimize heating, ventilation and air-conditioning (HVAC) strategies for energy management. Artificial Intelligence based techniques have been discussed for applications in IAQ, including energy forecasting, occupancy comfort prediction, occupancy detection, and fault detection [12]. However, selecting the most appropriate machine learning and deep learning models remains a challenge due to the wide range of algorithms used in building performance studies. Further developments and guidelines are needed to encourage best practices in model selection.

In some cases, sensors have been integrated into buildings to gather IAQ data and control HVAC systems to improve indoor conditions [13]. Artificial neural networks trained on monitored data have been used to regulate ventilation rates through IoT communication protocols.

As a response to the pressing need for an enhanced IAQ in buildings, several studies have delved into innovative strategies and technologies to ensure healthier indoor environments. Thus, Li et al. [14] introduced an innovative approach that leverages CFD in conjunction with a Back Propagation Neural Network (BPNN) integrated with a Particle

Swarm Optimizer (PSO) algorithm. This pioneering method swiftly predicts and optimizes IAQ conditions, while requiring only a limited number of CFD simulations. The results of this groundbreaking approach exhibited great promise, as the BPNN-PSO algorithm outperformed existing state-of-the-art IAQ control methods. It achieved a remarkable reduction in indoor air pollutant concentrations, reducing them by as much as 6.44%, while concurrently curtailing computational costs by up to 23.53%.

The research proposed by Ahtesham Bakht et al. [15] presents a promising approach to the predictive IAQ management through the utilization of deep learning techniques. While conventional deterministic methods for forecasting IAQ often require extensive calculations and specialized domain knowledge, deep learning-based methods have demonstrated excellent performance with significantly reduced computational requirements in recent studies. The authors introduce a hybrid deep learning framework which integrates multiple deep learning frameworks, including Convolution Neural Network, Long Short-Term Memory (LSTM), and Deep Neural Network. This framework is specifically designed to capture temporal patterns and informative features from indoor and outdoor air quality parameters, surpassing the capabilities of standalone deep learning models. The study's focus is on forecasting PM10 and PM2.5 concentrations. The demonstrated effectiveness of the hybrid framework in predicting future pollutant levels using historical air quality data is noteworthy.

Another noticeable study is the one reported by B. Lagesse et al. [16] which shed light on the significant gap in monitoring and regulating levels of the particulate matter PM2.5 within large office buildings. To address this critical issue, the authors designed statistical models using diverse modeling methods, including multiple linear regression, artificial neural networks, and LSTM. These models were meticulously trained using environmental and meteorological parameters as predictive factors to estimate PM2.5 concentrations in well-mixed indoor air. Impressively, the LSTM model emerged as the standout performer, with an interesting root mean square error. This model demonstrated remarkable accuracy in estimating PM2.5 levels even in the absence of ambient PM2.5 data.

In summary, this research not only addresses a critical gap in IAQ research by investigating cob buildings but also showcases the applicability of advanced deep learning models in the predictive IAQ management in such buildings. The insights gained from this study can contribute to a better understanding of the environmental and health implications of cob construction. Also, it can provide a valuable guidance for optimizing IAQ in these buildings during the first months following their delivery, enhancing occupants' comfort, health, and well-being.

## 2. Methodology

After reviewing the relevant recent literature, we developed an approach outlining our research procedures. The last lift of the studied prototype building being raised on the 33rd week of 2021, indoor/outdoor plasters and earthen floor were implemented, and carpentry installed. The CobBauge building was delivered on May 2022. The IAQ stations were then installed and data started to be recovered after 15 September 2022. The conceptual study strategy for this research is divided into four steps, as shown in Figure 1. Each step consists of several phases, all of which are covered in detail in the following sections. A summary of these phases is as follows:

1. Building construction and instrumentation: this phase provides a description of the building composition and the installation of air quality sensors.
2. Data collection: this phase describes the data recovery method.
3. Data preprocessing: for numerical treatment, the data were preprocessed by cleaning it, removing outliers, and aggregating it on an hourly basis.
4. Model selection: we evaluated the performance of the Long Short-Term Memory model (LSTM). LSTM is a type of recurrent neural network that can capture temporal dependencies in the data.

5. Model estimation: setting all the parameters required for the algorithm's execution constitutes the fifth step before evaluating the model.
6. Model evaluation: we assessed the performance of the models on the test set using various metrics such as the coefficient of determination (R-squared). We also visualized the predictions of the models and compared them with the actual data.

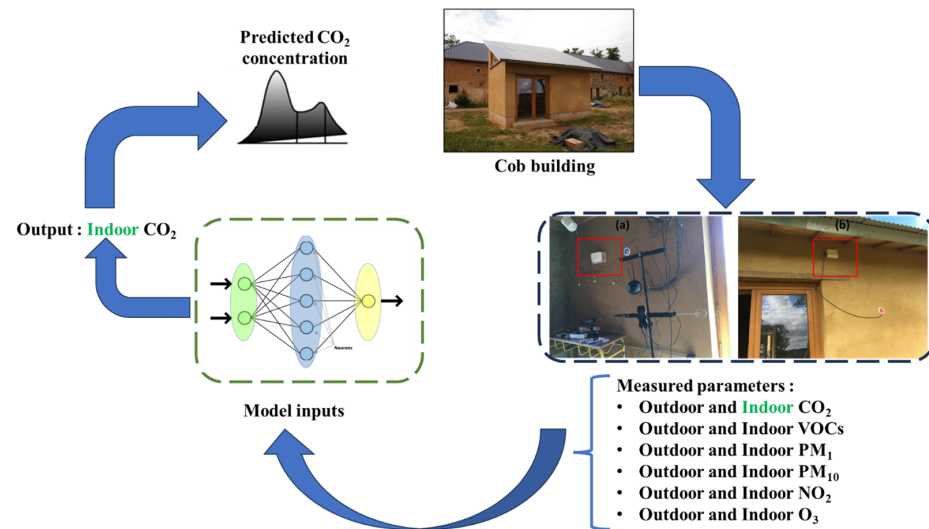


**Figure 1.** Conceptual study plan. Indoor (a) and outdoor ambiances (b) with the air quality stations (red squares).

### 2.1. Prototype Building Description

A cob building prototype was constructed within the Cotentin and Bessin Marshes Regional Natural Park's territory. This prototype building features an internal floor area of 13 m<sup>2</sup> and a total surface area of approximately 20 m<sup>2</sup>, with an earthen-based floor, see Figure 2. The construction of the prototype building employs a double-walling method, where cob and light earth naturally adhere to form a single wall. The typical wall thicknesses range from 50 to 70 cm. Specifically, the walls of this prototype are 50 cm thick on the south and west facades, and 70 cm thick on the east and north facades. While in the north and east facades, the walls are constituted by 40 cm cob (load bearing layer) and 30 cm light earth (insulating layer), in the south and west, facade are constituted by 25 cm cob and 25 cm light earth. The light earth layer is continuous on the outside of all walls to ensure better insulation performances. The walls were built using several lifts, each approximately 70 cm in height.



**Figure 2.** Global view of the CobBauge prototype building.



## 2.2. Indoor and Outdoor Air Quality Instrumentation

The CobBauge prototype building, designed for tertiary use, was equipped with instrumentation and subjected to monitoring. In this regard, two NEMo XT air quality stations from Ethera-labs were installed: one inside the prototype and the second one outside, as illustrated on Figure 3. These stations facilitate the measurement of various air quality parameters, including carbon dioxide (CO<sub>2</sub>), nitrogen dioxide (NO<sub>2</sub>), ozone (O<sub>3</sub>), volatile organic compounds (VOCs), fine particles (PM<sub>1</sub>, PM<sub>2.5</sub>, PM<sub>4</sub>, PM<sub>10</sub>), and relative humidity (RH). These stations measure also the temperature and the pressure.



**Figure 3.** Indoor (a) and outdoor air quality (b) stations.

For carbon dioxide, the detection method utilized non-dispersive infrared absorption spectroscopy (NDIR) within a measuring range spanning from 0 to 5000 ppm, with a resolution of 1 ppm and an uncertainty of  $\pm 30$  ppm or  $\pm 3\%$  of the measured value. Moreover, VOCs were detected using an electrochemical method, with a measuring range from 20 to 5 ppm, a resolution of 1 ppb, and an uncertainty of  $\pm 20$  ppb. The VOCs detected include formaldehyde and gases containing 1 to 4 carbon atoms (aldehydes, alcohols, etc.).

The temperature range covered by the monitoring system is from  $-55$  to  $125$  °C, with a precision of  $\pm 2$  °C. Relative humidity can be measured within the range of 5 to 95% with a precision of  $\pm 3\%$  (between  $\pm 11$  and 89%) and  $\pm 7\%$  outside this range.

Regarding fine particles (PM<sub>1</sub>, PM<sub>2.5</sub>, PM<sub>4</sub>, PM<sub>10</sub>), their detection relies on laser light diffraction. The measuring range extends from 0 to  $10 \mu\text{g}\cdot\text{m}^{-3}$ , with a resolution of  $1 \mu\text{g}\cdot\text{m}^{-3}$  and an uncertainty of  $\pm 10 \mu\text{g}\cdot\text{m}^{-3}$  ( $<100 \mu\text{g}\cdot\text{m}^{-3}$ ) and  $\pm 10\%$  ( $>100 \mu\text{g}\cdot\text{m}^{-3}$ ).

For nitrogen dioxide, an electrochemical method is employed, with a measuring range spanning from 1 to 17 ppm and an uncertainty of  $\pm 15$  ppb. Similarly, the detection of ozone also uses an electrochemical method, with a measuring range from 1 to 7600 ppb and an uncertainty of  $\pm 15$  ppb.

Data recorded by the various sensors constituting the air quality stations are collected at 10 min intervals between 15 September 2022 and 15 February 2023.

## 2.3. Artificial Neural Network Modelling

The literature frequently employs artificial neural networks (ANN) as a data-driven model for analysing building heating efficiency [17]. ANN models are derived from a simplified representation of biological neurons, which are translated into numerical forms. These neurons are expressed as mathematical entities capable of processing information [18]. The typical architecture of ANN models (as depicted in Figure 4) consists of three primary components:

- Synapses, which are connected to weights.
- A “summing junction” processing element that combines the synaptic weighting data input and adjusts them by incorporating a bias variable (bk).
- An activation function that governs the strength of the signal exiting the neuron.

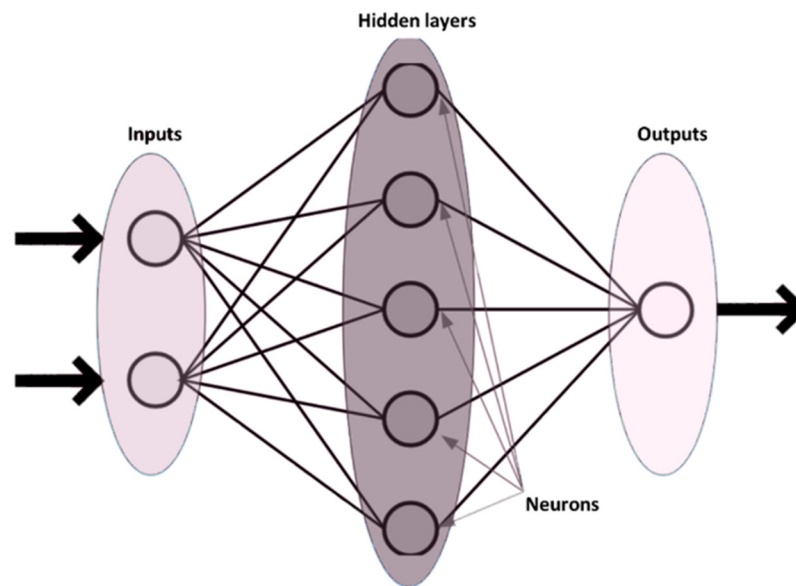


**Figure 4.** Simplified representation of an artificial neural network model.

The following equations can theoretically explain the neuron  $k$ :

$$u_k = \sum_{j=1}^m X_j w_{k,j} \quad (1)$$

$$v_k = u_k + b_k \quad (2)$$

where  $v_k$  is the weighted sum of the input signal modified using  $b_k$  and  $u_k$  is the linear yield of the original signal.

The output signal of the neuron  $k$  is determined by a series of mathematical equations called the activation function  $\varphi$ . The final output signal ( $y_k$ ), which is represented by the Equation (3), is obtained by adding the weighted and bias-corrected inputs. The sigmoid function, also known as the “gate”, is used to determine which information is allowed into the cell state.

$$Y_k = \varphi \left( \sum_{j=1}^m X_j w_{k,j} + b_k \right) \quad (3)$$

There are several types of neural network models used in indoor air quality prediction and analysis such as ANN, CNN, and LSTM. The LSTM model is often preferred for time series data due to its ability to retain long-term dependencies in sequential data [19,20], which can be important in predicting air quality as it often involves complex temporal patterns influenced by various factors. The LSTM’s architecture (Figure 5(left,right)), with its memory cells and ability to learn from sequences, can capture longer-term dependencies and nuances in time-series data, making it suitable for capturing the dynamics of air quality changes over time.

The LSTM model incorporates three key gates: the input gate, the forget gate, and the output gate. These gates play a pivotal role in governing the flow of information through the cell state by determining what information is added, what is forgotten, and what is outputted at each time step. The LSTM model, as described in reference [14], is defined by the following equations:

$$f_t = \sigma(W_f h_{t-1} + U_f X^t + b_f) \quad (4)$$

$$X^t = \sigma(W_X h_{t-1} + U_X X^t + b_X) \quad (5)$$

$$c'_t = \sigma(W_c h_{t-1} + U_c X^t + b_c) \quad (6)$$

$$c_t = f_t c_{t-1} + X^t c'_t \quad (7)$$

$$Y^t = \sigma(W_Y h_{t-1} + U_Y X^t + b_Y) \quad (8)$$

$$h_t = o_t \tanh(c_t) \quad (9)$$

The LSTM algorithm generates internal variables such as  $f_t$ ,  $X_t$ , and  $c'_t$ , which are utilized in the computation of  $c(t)$  and  $h(t)$  within the hidden layer. It is important to note that these equations must be recalculated for each upcoming time step, as the provided formulae are applicable to a single cycle. If the time series comprises three time steps, the equations will be solved three times. The weight matrices ( $W_f$ ,  $W_X$ ,  $W_Y$ ,  $W_c$ ,  $U_f$ ,  $U_X$ ,  $U_Y$ ,  $U_c$ ) and biases ( $b_f$ ,  $b_X$ ,  $b_Y$ ,  $b_c$ ) utilized in the model are constant and not time-dependent. Therefore, the same matrices are used to compute results for multiple time steps.

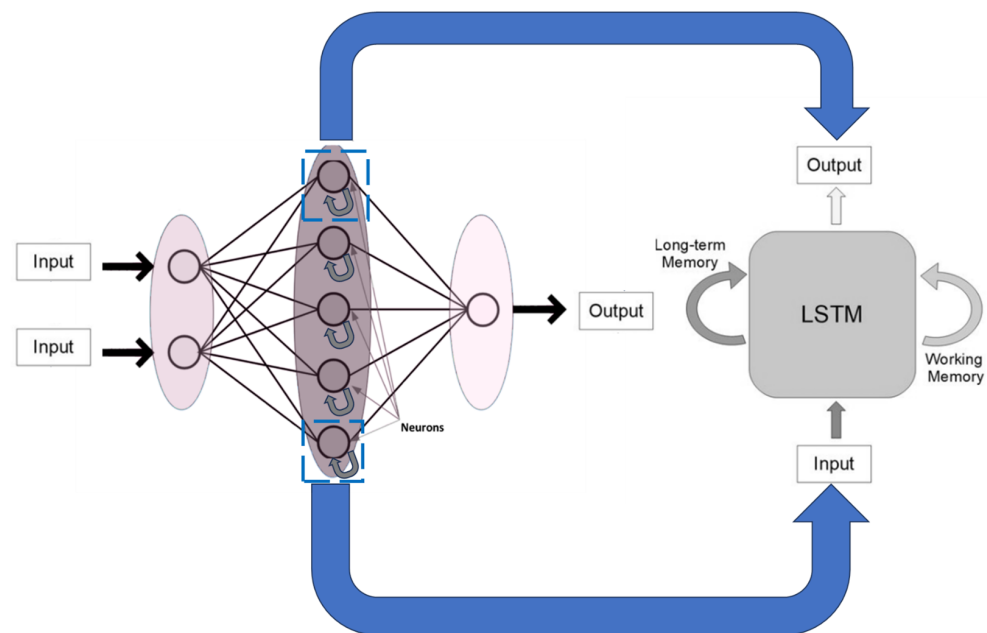


**Figure 5.** Structure of Recurrent Neural Network with hidden neurons (**left**) and an example of a long term memory cell's usual architecture (**right**).

The artificial neural network model is applied in three distinct stages. The first stage involves training the model to minimize the error function by adjusting the weight factors through a statistical comparison between experimental and simulation outputs. Subsequently, the model's results are assessed for their applicability using the determination coefficient ( $R^2$ ) and Root-Mean-Square Error (RMSE).

$$R^2 = 1 - \frac{\sum_{i=1}^n (\hat{y}_i - y_i)^2}{\sum_{i=1}^n (\bar{y}_i - y_i)^2} \quad (10)$$

$$RMSE = \sqrt{\frac{1}{n} \times \sum_{i=1}^n (\hat{y}_i - y_i)^2} \quad (11)$$

where  $y_i$  represents the observed values of the dependent variable.  $\hat{y}_i$  represents the predicted values of the dependent variable based on the regression model.  $n$  is the number of data points.  $\bar{y}_i$  represents the mean (average) of the observed values of the dependent variable.

The LSTM model excels at predicting future outcomes by analyzing historical data sequences. It learns patterns and trends from the input data and produces forecasts for upcoming time periods. The model is trained using the most recent data point, leveraging previously acquired patterns to predict outcomes for the subsequent time step. This iterative

process can be applied for as many future time steps as necessary. LSTM is a powerful tool widely employed in various applications, including language modeling, time series forecasting, and speech recognition, allowing it to predict future results based on past sequence data effectively.

Before being used as input features, the lagged time series data underwent pre-processing, including data normalization. This normalization step was applied. The purpose of normalization was to ensure that the input features were brought to a common scale, facilitating the model's training process. The division of the data into training (80%) and testing sets (20%) happened in the data partitioning function. This division ensured that the model was trained on a subset of the data and tested on another independent subset to evaluate its performance.

### 3. Results and Discussion

#### 3.1. Experimental Results

The experimental results reveal that the outdoor air temperature fluctuates between approximately  $-1$  and  $24$  °C, with pressure ranging from about 980 to 1050 mbar. Relative humidity varies between approximately 60 and 95%. Under these external conditions, the indoor air temperature of the building remains stable at around  $20$  °C even before the heating system is activated (started on 14 October). Figure 6 illustrates that the indoor temperature consistently remains within the comfort level throughout the entire study period. This clearly demonstrates that this prototype house is not prone to significant overheating risks, thanks to the behavior of its structural building materials during heatwaves and its location.

In terms of indoor relative humidity, Figure 6a indicates that RH oscillates around 80% (with occasional peaks) until November 30th. After this date, it decreases notably and fluctuates between 35 and 60%. This decrease can be attributed to the activation of a dehumidifier.

An indoor relative humidity approaching 80% is relatively high and suggests that the moisture balance is not fully achieved. This is likely due to the prototype cob walls not being completely dry. Such conditions may create a potential breeding ground for mold and bacteria if not addressed properly. It is generally accepted that the optimal range for indoor RH falls between 30 and 60% [21,22]. In this study, this range was achieved by installing a dehumidifier starting from 15 November. However, in real occupied buildings, an efficient ventilation system must also be designed to ensure adequate indoor RH [23].

Figure 6 indicates also that indoor pressure follows a similar trend to the outdoor pressure. This is noteworthy, as excessively low indoor pressure can potentially lead to the infiltration of outdoor pollutants into the indoor environment, while excessively high indoor pressure may cause the backdraft of combustion products and other indoor pollutants [24].

- **CO<sub>2</sub>**

In the outdoor environment, the levels of carbon dioxide vary between approximately 400 and 5000 ppm (5000 ppm being the detection limit of the air quality station), as shown in Figure 7. These CO<sub>2</sub> levels tend to be higher during the night and in the morning. It is worth noting that, in addition to photosynthesis, the increase in humidity during these periods can affect the measuring station. Therefore, absolute CO<sub>2</sub> values that appear significantly different from those observed in less humid conditions should be interpreted with caution. As the day progresses, photosynthesis occurs, and CO<sub>2</sub> levels tend to approach approximately 400 ppm.



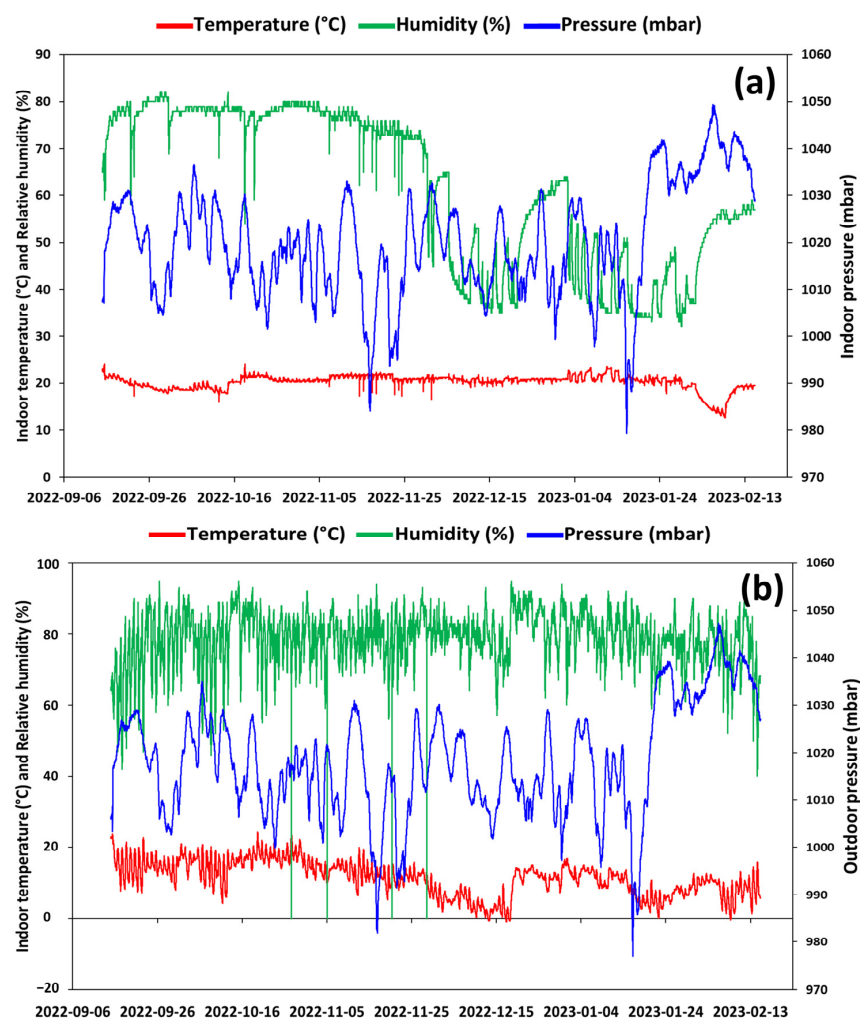


Figure 6. Indoor (a) and outdoor (b) temperature, pressure, and relative humidity of the cob prototype building.

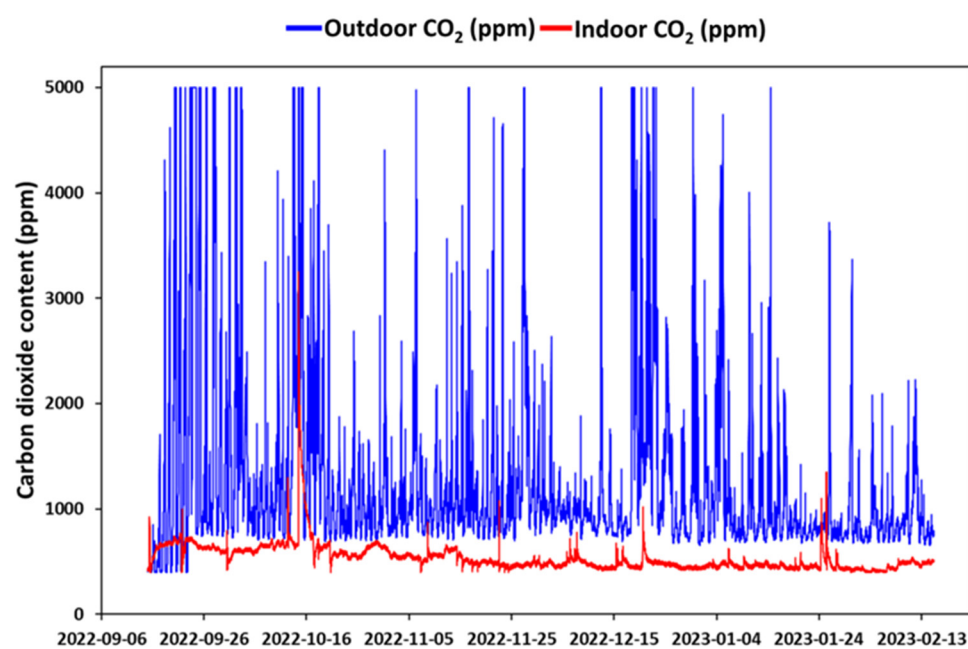


Figure 7. CobBauge prototype building indoor and outdoor carbon dioxide content.

Indoor carbon dioxide levels primarily range between 400 and 500 ppm throughout the testing period, with occasional spikes primarily linked to human presence within the building. These temporary spikes rapidly subside once the occupancy ceases. For instance, on October 14th, a spike reaching 3300 ppm is observed due to the presence of four individuals in the prototype building throughout the morning. To prevent such spikes, an efficient ventilation system tailored to occupancy patterns should be designed and implemented [23]. Elevated indoor CO<sub>2</sub> levels can lead to drowsiness, headaches, and other health issues.

Additionally, it is noticeable that the measured CO<sub>2</sub> levels are generally lower indoors across the entire considered period. In conclusion, Figure 7 indicates that indoor CO<sub>2</sub> concentration remains mostly below the standard limit of 1000 ppm recommended by European guidelines [25]. A description of the indoor CO<sub>2</sub> concentration is given in Table 1.

**Table 1.** Indoor CO<sub>2</sub> dataset statistical description.

Data	Mean	Standard Deviation	Max	Min
Concentration of CO <sub>2</sub> [ppm]	537	146	2716	137

#### • VOCs

Construction products that contain organic materials, such as cob construction with a high content of vegetable fibers, can emit volatile organic compounds. The presence of these compounds in a building often results in odors that can be irritating. The perception of unpleasant odors tends to increase as temperatures rise due to solar radiation or during warmer months, especially when building ventilation is limited [26]. Apart from product emissions, several other factors, including relative humidity, air exchange rates, and temperature, can influence the levels of VOCs inside buildings [27]. VOCs are a common indoor air pollutant that can have adverse health effects [28], making their control critically important.

In the present study, outdoor VOCs level ranged from approximately 5 to 50 ppb but were primarily between 10 and 20 ppb. A spike was observed during the initial hours of measurement, which resulted from the transportation of the air quality stations in a car from the office to the experimentation site. These spikes rapidly declined as the stations were installed on-site on 15 September.

In the indoor environment, VOCs concentrations remained close to zero until October 14th, when four individuals were active in the prototype building for half a day. After that date, VOCs level remained quite low until December 8th, as shown in Figure 8. Following that date, a noticeable increase in VOCs level can be observed, likely attributed to the reduction in indoor relative humidity, as depicted in Figure 6. The maximum concentration of VOCs is reached several dozen days later, showing a delayed response to the decrease in indoor humidity. Moreover, the higher VOCs concentration persists at an elevated level [28].

Subsequently, after that date, the level of volatile organic compounds fluctuated between approximately 0 and 30 ppb, approaching the range of outdoor values. The low levels of VOCs observed during the experiment suggest that there may be no significant indoor sources of VOCs, or any potential sources are effectively controlled or removed by the natural ventilation [29].

#### • Particulate matter

The levels of particulate matter (PM<sub>1</sub> and PM<sub>10</sub>) vary between approximately 0 and 10 µg/m<sup>3</sup>, with occasional spikes, as seen in the data. These spikes in particulate matter concentration may be attributed to local sources of pollution in the vicinity of the monitoring site. For instance, the spike observed on 29 November 2022, could be linked to nearby activities such as agricultural operations, increased traffic on neighboring roads, or industrial activities, especially considering the presence of a materials preparation

plant nearby. Two significant peaks observed indoors on 16 October 2022 and 24 January 2023, are associated with a human presence. These peaks resulted from the movement of individuals on the earthen floor, which was already damaged, causing the release of substantial quantities of fine particles.

In general, the concentration of particulate matter tends to be relatively lower indoors compared to outdoors. However, the trends are similar, although with a slight time delay, as indicated in Figures 9 and 10.

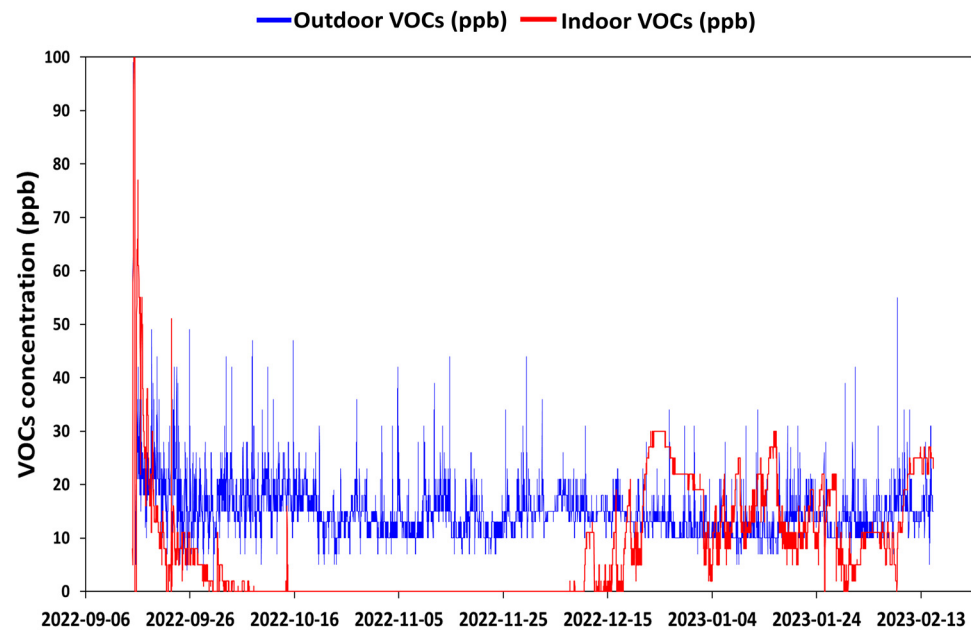


Figure 8. CobBauge prototype building indoor and outdoor volatile organic compounds.

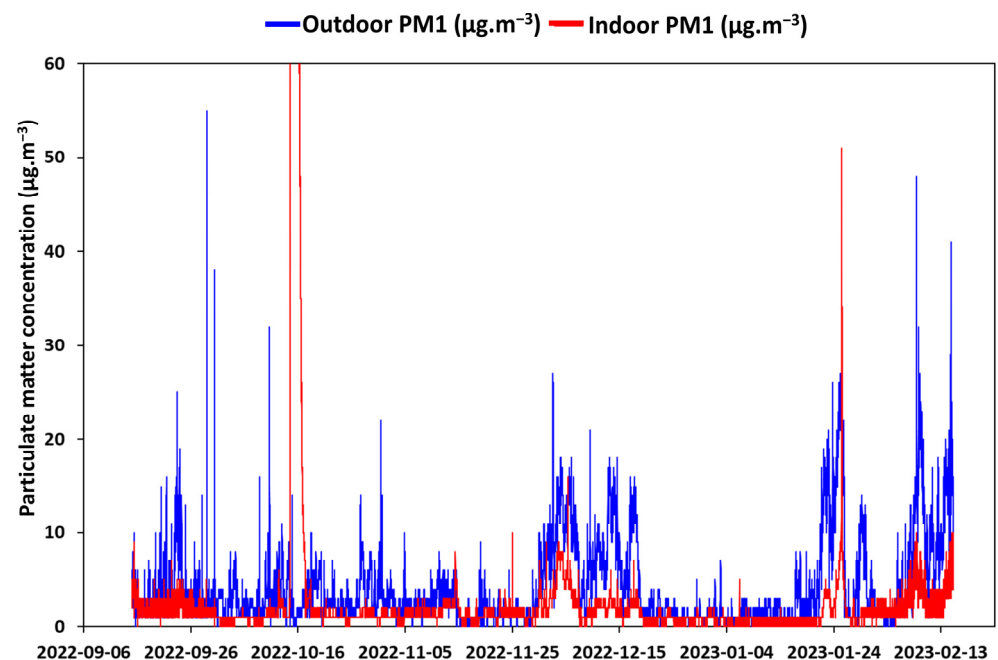


Figure 9. CobBauge prototype building indoor and outdoor PM1 concentration.

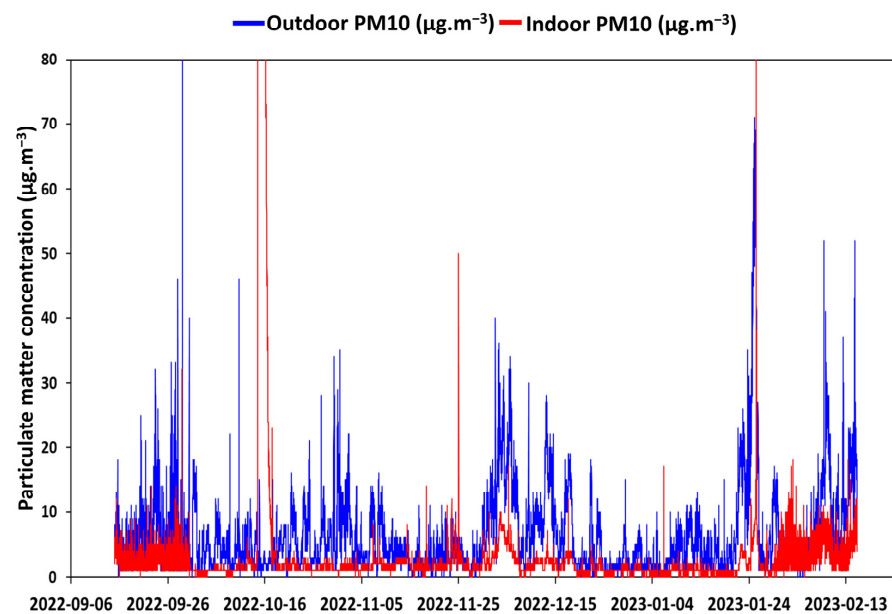


Figure 10. CobBauge prototype building indoor and outdoor PM10 concentration.

- **NO<sub>2</sub> and O<sub>3</sub>**

It is indeed essential to note that nitrogen dioxide is a chemical compound known to have adverse health effects, particularly on individuals with pre-existing respiratory conditions [30].

In the current study, the outdoor level of NO<sub>2</sub> was found to range between approximately 10 and 30 ppb, with occasional peaks reaching approximately 0 to 55 ppb. On the other hand, ozone levels in the outdoor environment primarily fluctuated between approximately 0 and 40 ppb.

Indoors, the level of NO<sub>2</sub> displayed a wider range, varying between 0 and 20 ppb but mainly oscillating between 5 and 15 ppb from 15 September to 30 November. After 30 November, NO<sub>2</sub> levels became negligible, except for a brief period between February 5th and 8th, which coincided with the switch-off of the heating system and the presence of a dehumidifier, as illustrated in Figure 11.

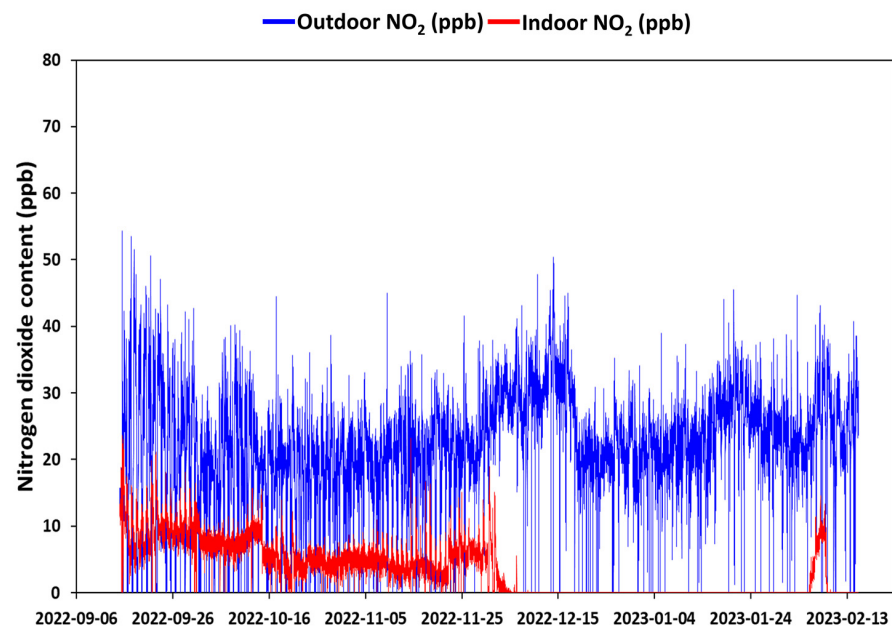


Figure 11. CobBauge prototype building indoor and outdoor nitrogen dioxide level.



In contrast,  $O_3$  concentrations indoors were relatively negligible until 30 November, except for occasional peaks associated with human presence in the building. Human presence typically involves the opening of doors and a decrease in relative humidity. After 30 November, ozone content indoors varied between approximately 0 and 10 ppb, as shown in Figure 12.

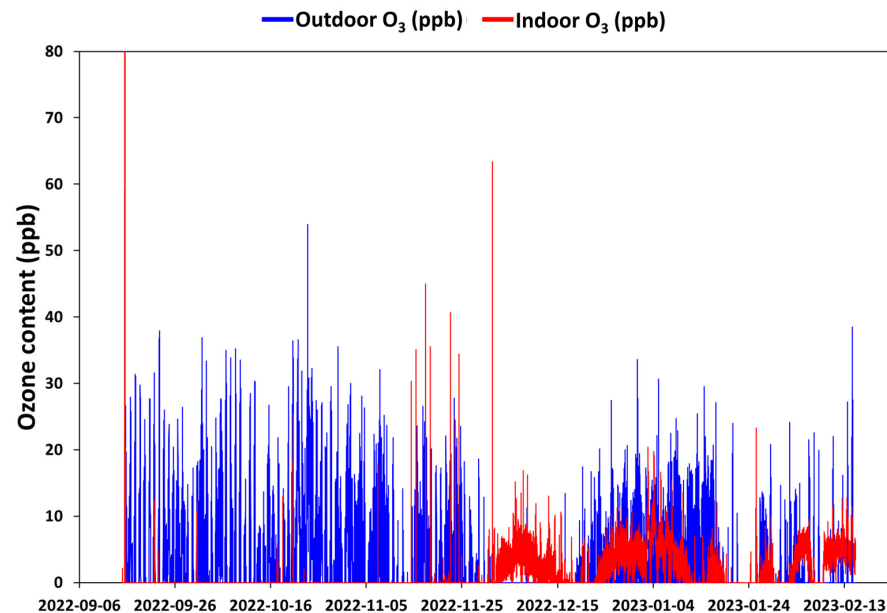


Figure 12. CobBauge prototype building indoor and outdoor ozone level.

These figures highlight that indoor levels of both  $NO_2$  and  $O_3$  are generally lower than those observed outdoors. Furthermore, the operation of the dehumidifier had a noticeable impact on indoor air quality, affecting the levels of  $NO_2$  and  $O_3$ . Importantly, these indoor levels fall within the recommended guidelines set by various health organizations. Depending on ventilation rates, mean indoor  $O_3$  content can range from 0 to 60 ppb. The European accepted levels for  $NO_2$  and  $O_3$  during a 1 h period are equal to 100 ppb [31–33].

The experimental results indicate that indoor air quality is marked by elevated relative humidity, possibly attributed to the continuous release of moisture from the cob construction into the indoor environment, even after 13 months from the last lift's implementation [34]. Additionally, the levels of carbon dioxide, volatile organic compounds, particulate matter, nitrogen dioxide, and ozone appear to be lower indoors than outdoors, although the impact of the damaged earthen floor and the dehumidifier's operation has been noted. Moreover, occasional spikes in these parameters, resulting from occupancy and indoor environmental variations, have been observed. However, when dealing with buildings evolving in conditions different from those considered in the present study, the RH and pollutants absolute values reported in the present study should be considered carefully. In such studies, attention should be paid to the mixtures' composition and preparation, implementation method and conditions, weather conditions, and use scenarios. These findings underscore the importance of monitoring and managing indoor air quality in cob buildings to ensure occupant comfort and health.

### 3.2. Numerical Results

In Figure 13a, we present a comparison between the in situ  $CO_2$  measurements obtained from the air quality station and the predicted  $CO_2$  evolution using the LSTM model. Additionally, a regression vector with an  $R^2$  value of 0.984 is calculated and a Pearson correlation map is included, see Figure 14. An RMSE value of 15.94 is also calculated. The high R-squared value indicates that the model explains a significant proportion of the variance in the data. Figure 13a demonstrates the validation of the LSTM model, which accurately detected the peak in  $CO_2$  concentration that occurred on 14 October. Figure 13b

displays the predicted CO<sub>2</sub> data beyond the testing period. LSTM was able to validate CO<sub>2</sub> by considering a sequence of past CO<sub>2</sub> concentration data as input and using this data to learn patterns and trends. Once trained, the model generated predictions for future CO<sub>2</sub> concentrations by incorporating the most recent CO<sub>2</sub> concentration data point and applying the previously learned patterns to predict the next time step. This process could be repeated for as many future time steps as needed.

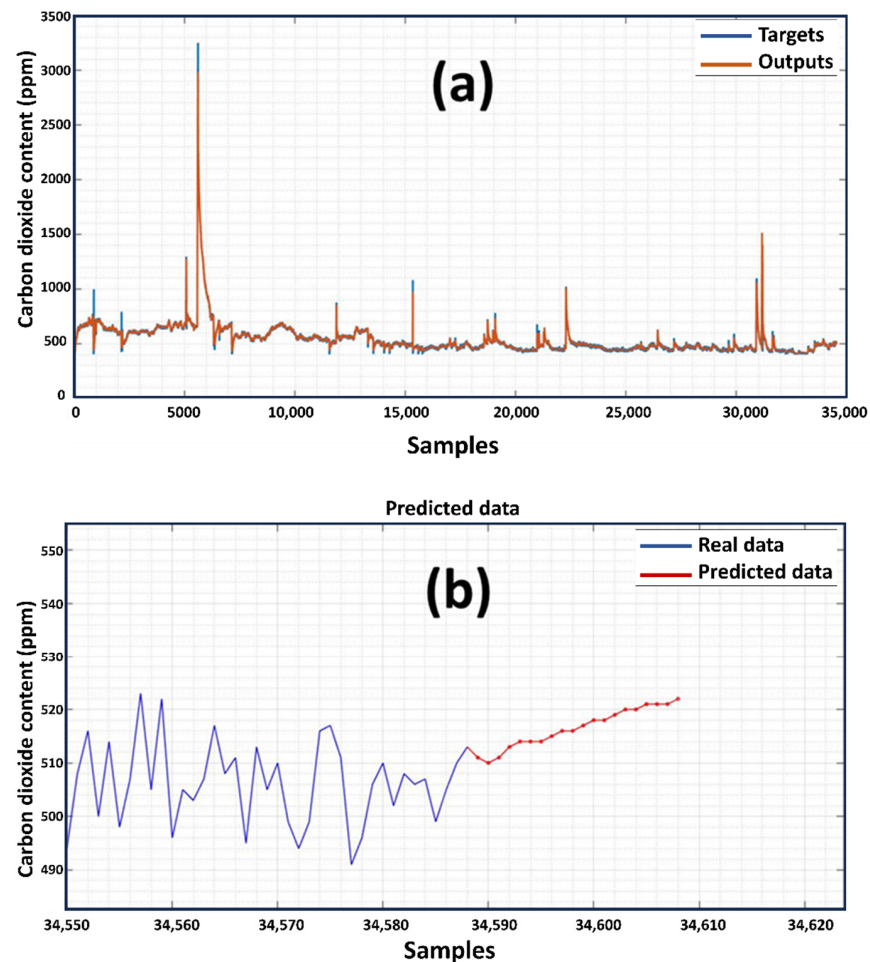


Figure 13. Model validation (a) and predicted CO<sub>2</sub> concentration (b).

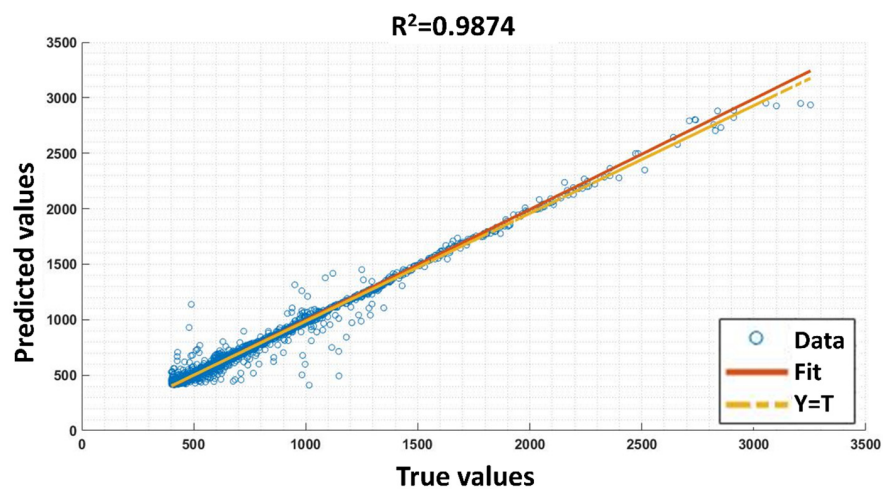


Figure 14. Pearson correlation map.

To predict upcoming CO<sub>2</sub> concentrations beyond the testing period, LSTM employed the same approach as in the validation process. It considered the most recent CO<sub>2</sub> concentration data point and used the previously learned patterns to predict future CO<sub>2</sub> concentrations for as many time steps as desired. This allowed for reliable predictions of future CO<sub>2</sub> concentrations based on historical sequence data.

Based on our predictions using LSTM, it appears that the evolution of CO<sub>2</sub> concentrations inside the building is expected to fluctuate between 510 and 530 ppm in the future, consistently remaining within a favorable range. Furthermore, LSTM's ability to forecast future CO<sub>2</sub> concentrations based on historical data can be valuable for building managers and facility operators seeking to optimize indoor air quality, ventilation, and energy efficiency.

#### 4. Conclusions

The present study has provided valuable insights into the indoor air quality (IAQ) of a cob prototype building through a combination of experimental measurements and numerical analysis. This research addresses a gap in the existing body of knowledge regarding the IAQ of cob buildings and contributes to a better understanding of the key pollutants that impact occupants' health. This research was particularly focused on the IAQ in a cob building during the first few months following its delivery. The in situ measurements conducted during this study revealed several important findings regarding the indoor ambience:

- Air temperature was maintained within the human comfort zone.
- Relative Humidity (RH) levels were relatively high, approaching 80%, which may be attributed to the characteristics of cob construction. The cob walls are supposed to be still wet and their practical water content level was not completely reached [35]. This may suppose the use of a drying fan for a longer period of time. Otherwise, prefabricating cob before its implementation makes sense.
- Carbon Dioxide (CO<sub>2</sub>) levels remained between 400 and 500 ppm throughout the testing period, with occasional spikes associated with human presence that quickly dissipated. The indoor CO<sub>2</sub> concentration generally fell below the standard limit of 1000 ppm recommended by European guidelines.
- Low levels Volatile Organic Compounds (VOCs) were observed indoors, suggesting the absence of significant indoor sources of VOCs and the potential effectiveness of the natural ventilation.
- Particulate Matter (PM1 and PM10): human presence and walking on a damaged earthen floor raised significant quantities of fine particles (PM1 and PM10). Otherwise, their indoor concentration followed similar trends to outdoor levels, with a slight time delay.
- Nitrogen Dioxide (NO<sub>2</sub>) and Ozone (O<sub>3</sub>) levels were generally lower than those measured outdoors. The operation of the dehumidifier had an impact on indoor NO<sub>2</sub> and O<sub>3</sub> levels, but these remained within the recommended guidelines (100 ppb).

Overall, the majority of the studied parameters suggest that cob buildings can provide good IAQ even during the first few months following their delivery. However, challenges such as fluctuating indoor RH and occasional pollutant peaks need to be addressed to mitigate potential risks to human health. To achieve consistently good IAQ, an appropriate mechanical ventilation system may be necessary. Also, the eventual degradation of earthen floors and their eventual impact on the IAQ should be considered when designing such buildings. The use of the Long Short-Term Memory model for predicting pollutant concentrations may be a valuable tool for building managers and facility operators aiming to optimize IAQ.

Further research exploring IAQ in a completely dry cob building under use may be performed. Also, other studies considering other soils and vegetal straws, other regions and climates can also be carried out.

**Author Contributions:** Conceptualization, K.T., M.L.G., F.S. and S.G.; methodology, K.T., M.-H.B., Y.E.M. and M.L.G.; investigation, data curation, and formal analysis, K.T., M.-H.B. and Y.E.M.; writing—original draft preparation, K.T., M.-H.B. and Y.E.M.; writing—review and editing, K.T., M.-H.B., Y.E.M., F.S. and S.G.; funding acquisition, S.G. and F.S. All authors have read and agreed to the published version of the manuscript.

**Funding:** The results presented in this article were obtained in the framework of the collaborative project CobBauge, funded by the European cross-border cooperation program INTERREG V France (Manche/Channel) England.

**Data Availability Statement:** The experimental and computational data presented in this present paper are available from the corresponding author upon request.

**Conflicts of Interest:** The authors declare no conflict of interest.

## References

1. Mannan, M.; Al-Ghamdi, S.G. Indoor Air Quality in Buildings: A Comprehensive Review on the Factors Influencing Air Pollution in Residential and Commercial Structure. *Int. J. Environ. Res. Public Health* **2021**, *18*, 3276. [\[CrossRef\]](#) [\[PubMed\]](#)
2. Apte, K.; Salvi, S. Household air pollution and its effects on health. *F1000Research* **2016**, *5*, 2593. [\[CrossRef\]](#)
3. Sisask, M.; Värnik, P.; Värnik, A.; Apter, A.; Balazs, J.; Balint, M.; Bobes, J.; Brunner, R.; Corcoran, P.; Cosman, D.; et al. Teacher satisfaction with school and psychological well-being affects their readiness to help children with mental health problems. *Health Educ. J.* **2014**, *73*, 382–393. [\[CrossRef\]](#)
4. Vilčeková, S.; Apostoloski, I.Z.; Mečiarová, L.; Burdová, E.K.; Kiseľák, J. Investigation of indoor air quality in houses of Macedonia. *Int. J. Environ. Res. Public Health* **2017**, *14*, 37. [\[CrossRef\]](#)
5. Wei, G.; Yu, X.; Fang, L.; Wang, Q.; Tanaka, T.; Amano, K.; Yang, X. A review and comparison of the indoor air quality requirements in selected building standards and certifications. *Build. Environ.* **2022**, *226*, 109709. [\[CrossRef\]](#)
6. Wu, P.; Fang, Z.; Luo, H.; Zheng, Z.; Zhu, K.; Yang, Y.; Zhou, X. Comparative analysis of indoor air quality in green office buildings of varying star levels based on the grey method. *Build. Environ.* **2021**, *195*, 107690. [\[CrossRef\]](#)
7. Wei, W.; Ramalho, O.; Mandin, C. Indoor air quality requirements in green building certifications. *Build. Environ.* **2015**, *92*, 10–19. [\[CrossRef\]](#)
8. Xiong, Y.; Krogmann, U.; Mainelis, G.; Rodenburg, L.A.; Andrews, C.J. Indoor air quality in green buildings: A case-study in a residential high-rise building in the northeastern United States. *J. Environ. Sci. Health Part A Toxic/Hazard. Subst. Environ. Eng.* **2015**, *50*, 225–242. [\[CrossRef\]](#)
9. Akom, J.B.; Sadick, A.M.; Issa, M.H.; Rashwan, S.; Duhoux, M. The indoor environmental quality performance of green low-income single-family housing. *J. Green Build.* **2018**, *13*, 98–120. [\[CrossRef\]](#)
10. Arundel, A.V.; Sterling, E.M.; Biggin, J.H.; Sterling, T.D. Indirect health effects of relative humidity in indoor environments. *Environ. Health Perspect.* **1986**, *65*, 351–361. [\[CrossRef\]](#) [\[PubMed\]](#)
11. Darling, E.K.; Cros, C.J.; Wargocki, P.; Kolarik, J.; Morrison, G.C.; Corsi, R.L. Impacts of a clay plaster on indoor air quality assessed using chemical and sensory measurements. *Build. Environ.* **2012**, *57*, 370–376. [\[CrossRef\]](#)
12. Tien, P.W.; Wei, S.; Darkwa, J.; Wood, C.; Calautit, J.K. Machine learning and deep learning methods for enhancing building energy efficiency and indoor environmental quality—A review. *Energy AI* **2022**, *10*, 100198. [\[CrossRef\]](#)
13. Tagliabue, L.C.; Cecconi, F.R.; Rinaldi, S.; Ciribini, A.L.C. Data driven indoor air quality prediction in educational facilities based on IoT network. *Energy Build.* **2021**, *236*, 110782. [\[CrossRef\]](#)
14. Li, L.; Zhang, Y.; Fung, J.C.; Qu, H.; Lau, A.K. A coupled computational fluid dynamics and back-propagation neural network-based particle swarm optimizer algorithm for predicting and optimizing indoor air quality. *Build. Environ.* **2022**, *207*, 108533. [\[CrossRef\]](#)
15. Bakht, A.; Sharma, S.; Park, D.; Lee, H. Deep Learning-Based Indoor Air Quality Forecasting Framework for Indoor Subway Station Platforms. *Toxics* **2022**, *10*, 557. [\[CrossRef\]](#)
16. Lagesse, B.; Wang, S.; Larson, T.V.; Kim, A.A. Predicting PM2.5 in well-mixed indoor air for a large office building using regression and artificial neural network models. *Environ. Sci. Technol.* **2020**, *54*, 15320–15328. [\[CrossRef\]](#)
17. Adibimanesh, B.; Polesek-Karczewska, S.; Bagherzadeh, F.; Szczuko, P.; Shafighfard, T. Energy consumption optimization in wastewater treatment plants: Machine learning for monitoring incineration of sewage sludge. *Sustain. Energy Technol. Assess.* **2023**, *56*, 103040. [\[CrossRef\]](#)
18. Haykin, S.S. *Neural Networks and Learning Machines*, 3rd ed.; Prentice-Hall: New York, NY, USA; Munich, Germany, 2009.
19. Bagherzadeh, F.; Shafighfard, T.; Khan, R.M.A.; Szczuko, P.; Mieloszyk, M. Prediction of maximum tensile stress in plain-weave composite laminates with interacting holes via stacked machine learning algorithms: A comparative study. *Mech. Syst. Signal Process.* **2023**, *195*, 110315. [\[CrossRef\]](#)
20. Seo, B.; Yoon, Y.; Lee, K.H.; Cho, S. Comparative Analysis of ANN and LSTM Prediction Accuracy and Cooling Energy Savings through AHU-DAT Control in an Office Building. *Buildings* **2023**, *13*, 1434. [\[CrossRef\]](#)



21. Overen, O.K.; Meyer, E.L.; Makaka, G. Indoor Daylighting and Thermal Response of a Passive Solar Building to Selective Components of Solar Radiation. *Buildings* **2021**, *11*, 34. [\[CrossRef\]](#)
22. Bouasria, M.; Benzaama, M.H.; Pralong, V.; El Mendili, Y. Mechanical and hygrothermal performance of fly-ash and seashells concrete: In situ experimental study and smart hygrothermal modeling for Normandy climate conditions. *Arch. Civ. Mech. Eng.* **2022**, *22*, 100. [\[CrossRef\]](#)
23. Hema, C.; Messan, A.; Lawane, A.; Soro, D.; Nshimiyimana, P.; van Moeseke, G. Improving the thermal comfort in hot region through the design of walls made of compressed earth blocks: An experimental investigation. *J. Build. Eng.* **2021**, *38*, 102148. [\[CrossRef\]](#)
24. Fu, N.; Kim, M.K.; Chen, B.; Sharples, S. Investigation of outdoor air pollutant, PM<sub>2.5</sub> affecting the indoor air quality in a high-rise building. *Indoor Built Environ.* **2022**, *31*, 895–912. [\[CrossRef\]](#)
25. EN 13779; Ventilation for Non-Residential Buildings—Performance for Ventilation and Room Conditioning Systems. European Committee for Standardization: Brussels, Belgium, 2008.
26. Tham, S.; Thompson, R.; Landeg, O.; Murray, K.A.; Waite, T. Indoor temperature and health: A global systematic review. *Public Health* **2020**, *179*, 9–17. [\[CrossRef\]](#)
27. Kostyrko, K.; Wargocki, P. *Measurements of Odours and Perceived Indoor Air Quality in Buildings*; Scientific Studies Research Building Institute; ITB Publishing: Warsaw, Poland, 2012.
28. Piasecki, M.; Kostyrko, K.B.; Goljan, A. The Ability to Control VOC Emissions from Multilayer Building Materials. *Appl. Sci.* **2021**, *11*, 4806. [\[CrossRef\]](#)
29. Willem, H.; Hult, E.L.; Hotchi, T.; Russell, M.L.; Maddalena, R.L.; Singer, B.C. Ventilation Control of Volatile Organic Compounds. In *New, U.S. Homes: Results of a Controlled Field Study in Nine Residential Units*; LBNL-6022E; Lawrence Berkeley National Laboratory: Berkeley, CA, USA, 2013; pp. 1–64.
30. Gubb, C.; Blanus, T.; Griffiths, A.; Pfrang, C. Potted plants can remove the pollutant nitrogen dioxide indoors. *Air Qual. Atmos. Health* **2022**, *15*, 479–490. [\[CrossRef\]](#)
31. Zhou, S.; Young, C.J.; VanderBoer, T.C.; Kahan, T.F. Role of location, season, occupant activity, and chemistry in indoor ozone and nitrogen oxide mixing ratios. *Environ. Sci. Process. Impacts* **2019**, *21*, 1374–1383. [\[CrossRef\]](#)
32. Zhang, J.F.; Lioy, P.J. Ozone In Residential Air—Concentrations, I/O Ratios, Indoor Chemistry, And Exposures. *Indoor Air* **1994**, *4*, 95–105. [\[CrossRef\]](#)
33. Braun, M.; Klingelhöfer, D.; Müller, R.; Groneberg, D.A. The impact of second-hand smoke on nitrogen oxides concentrations in a small interior. *Sci. Rep.* **2021**, *11*, 11703. [\[CrossRef\]](#) [\[PubMed\]](#)
34. Touati, K.; Le Guern, M.; El Mendili, Y.; Azil, A.; Streiff, F.; Carfrae, J.; Fox, M.; Goodhew, S.; Boutouil, M. Earthen-based building: In-situ drying kinetics and shrinkage. *Const. Build. Mater.* **2023**, *369*, 130544. [\[CrossRef\]](#)
35. Touati, K.; Benzaama, M.-H.; El Mendili, Y.; Le Guern, M.; Streiff, F.; Goodhew, S. Hygrothermal and Economic Analysis of an Earth-Based Building Using In Situ Investigations and Artificial Neural Network Modeling for Normandy's Climate Conditions. *Sustainability* **2023**, *15*, 13985. [\[CrossRef\]](#)

**Disclaimer/Publisher's Note:** The statements, opinions and data contained in all publications are solely those of the individual author(s) and contributor(s) and not of MDPI and/or the editor(s). MDPI and/or the editor(s) disclaim responsibility for any injury to people or property resulting from any ideas, methods, instructions or products referred to in the content.